Carbohydrate Polymers 17 (1992) 209–220

Rheology of xanthan and scleroglucan in synthetic seawater

B. T. Stokke, A. Elgsaeter

Norwegian Biopolymer Laboratory, Department Physics and Mathematics, University of Trondheim, NTH, N-7034 Trondheim, Norway

E. Ø. Bjørnestad & T. Lund

Statoil, PO Box 300 Forus, N-4000 Stavanger, Norway

(Received 1 November 1990; revised version received 28 January 1991; accepted 31 January 1991)

Rheological characterization of xanthan from three different sources and scleroglucan from two different sources has been carried out using synthetic seawater as solvent. The measurements spanned temperatures from 20°C to 70°C, shear rates from 0·5 s^{-1} to 100 s^{-1} and polymer concentrations from 30 μg/ml to 1 mg/ml. The observed difference in effectiveness of increasing solution viscosity at low shear is quantitated in terms of the intrinsic viscosity $[\eta]$. Scleroglucan A was found to be the most effective with $[\eta]$ = 14 000 ml/g and xanthan B the least effective with $[\eta]$ = 5060 ml/g, both at T = 20°C. The temperature coefficients of the intrinsic viscosities, $\partial \ln[\eta]/\partial T$, was found to lie in the range $\partial \ln[\eta]/\partial T = -(9\text{–}19)\ 10^{-3}\ K^{-1}$ for the xanthans and $\partial \ln[\eta]/\partial T = -1{\cdot}9\ 10^{-3}\ K^{-1}$ for the scleroglucans. These findings were interpreted in terms of a decrease in chain stiffness with temperature. Assuming a worm-like chain model the temperature coefficients of the persistence length q were $\partial \ln q/\partial T = -(9{\cdot}4\text{–}21)\ 10^{3}\ K^{-1}$ and $-2{\cdot}1\ 10^{-3}\ K^{-1}$ for xanthans and scleroglucans, respectively. The viscosity at low shear rate in the semi-dilute concentration range is accounted for in terms of entanglement of overlapping chains. The lowering of viscosity in the semi-dilute concentration range associated with increasing shear rate is observed for smaller shear rates than in the dilute regime. Thus the decrease in entanglement starts at lower shear rate than orientational effects at the molecular level.

INTRODUCTION

Xanthan gum and scleroglucan are high molecular weight polysaccharides of potential use in polymer flooding and permeability modification of oil containing formations (Davison & Mentzer, 1982; Holzwarth 1985). The high viscosity of these polymers at low solution concentrations is due to both high molecular weight and high structural chain rigidity. The chain rigidity of polymers can be quantitated in terms of the persistence length for a worm-like chain model, which for these two polymers exceeds 100 nm. The molecular reason for this high stiffness is most likely the multistranded nature of the polymers. The prevalance of the ordered, probably double-stranded, conformation of xanthan at high salt concentrations and low temperature, and the triple-stranded conformation of scleroglucan, also provide a molecular basis for the enhanced long-term stability of these polymers under harsh thermal conditions compared to single-stranded polysaccharides.

The molecular interpretation of apparently comparable experimental data on xanthan differ among various research groups. This can be exemplified by the intrinsic viscosity data of Milas and coworkers (Milas & Rinaudo, 1986; Milas *et al.*, 1986) for a presumably single-stranded xanthan sample which did not differ significantly from the data of Sato *et al.* (1984*a*) for a sample interpreted as being double-stranded xanthan. Furthermore, there are reported differences in rheological properties both between commercial xanthans and between scleroglucan preparations (Sandford *et al.*, 1977; Smith *et al.*, 1981; Lange, 1988). Such studies often extend to polymer concentrations where intermolecular effects dominate. Rheological comparisons of different polymer batches at solvent conditions used in oil fields constitute the routine quality performance tests in most oil companies and are a necessary

Carbohydrate Polymers 0144-8617/91/$03.50

evaluation prior to pilot polymer flooding tests. The salt concentrations used in such product screening are generally selected to match those used in the injection fluid. They differ from the conditions used in the experiments cited above. In these experiments the polymer solutions were prepared in solvent ranging from freshwater to synthetic seawater with about 3·5% total dissolved salts. The advantage of the stiff-chain biopolymers compared to synthetic polymers in maintaining high viscosities increases with increasing salt concentration.

The temperature dependence of xanthan solution viscosity has been the subject of several reports (Sandford *et al.*, 1977; Whitcomb & Macosko, 1978; Launay *et al.*, 1984; Speers & Tung, 1986; Rochefort & Middleman, 1987). Temperature effects are in most cases reported as the temperature dependence of the solution viscosity at constant shear rate $\dot{\gamma}$ and it is often classified qualitatively as either 'not typical' or 'unusual' for dilute or semi-dilute polymer solutions. Such data reveal that, depending on the product origin, the viscosity may be an increasing as well as a decreasing function of temperature (Sandford *et al.*, 1977). The sign of this temperature effect depends on the salt concentration even for preparations that all correspond to the ordered conformation (Holzwarth, 1976). The viscosity decreases with increasing temperature at a shear rate of $\dot{\gamma} = 14\ s^{-1}$, while the viscosity is independent of temperature while evaluated at $\dot{\gamma} = 127\ s^{-1}$ and even increases when measured at $\dot{\gamma} = 571\ s^{-1}$ (Morris *et al.*, 1977). Similar shear rate effects on the temperature dependence of the relative viscosity for a 0·8 mg/ml xanthan solution in 2% NaCl is reported by Launay *et al.* (1984). This illustrates that the temperature influence on viscosity depends on the shear rate selected. Furthermore, the temperature dependence was found to diminish when the xanthan concentration of 1 mg/ml was considered, whereas increasing the polymer concentration to 10 mg/ml yielded a viscosity increase with increasing temperature (Speers & Tung, 1986). Dependence of the acetate and pyruvate level on the viscosity change occurring upon addition of salt (Smith *et al.*, 1981) suggests that the pyruvate and acetate substitution of the side-chains influence the rheology of xanthan in the semi-dilute concentration range. There are fewer reports on the temperature of aqueous scleroglucan solutions. Bluhm *et al.* (1982) report that the specific viscosity η_{sp} of a scleroglucan solution was independent of temperature (shear rate not specified in the employed capillary viscometer) in the range 10–70°C whereas a divergence in η_{sp}/c induced by gelation was reported on cooling below 10°C. Rivenq *et al.* (1989) report that the viscosity of a 2 mg/ml scleroglucan solution measured at a shear rate $\dot{\gamma} = 1000\ s^{-1}$ declines slightly on increasing temperature up to 115°C. At higher temperatures a marked drop in viscosity is encountered. This drop was attributed to melting of the triple-helical structure into its three subunits.

The aim of this study is to compare rheological properties of three xanthan samples from two different commercial sources, one xanthan sample fermented on pilot scale at Statoil, and two scleroglucan samples. All these samples except one of the scleroglucan samples are available as pasteurized fermentation broths. Samples for measurements were prepared by dispersion of the broths in 3·5% synthetic brine thus avoiding drying of the polymers. Comparison of the rheological properties of the polymers from various sources was carried out by analyzing data from rheological measurements covering a range of polymer concentrations in both the dilute and semi-dilute regime. The experiments have been performed at various solution shear rates and temperatures. The intrinsic viscosity $[\eta]$, Huggins constant and shear rate $\dot{\gamma}_c$ denoting the onset of the decrease in $[\eta]$ at increasing shear rate, will be used as parameters describing dilute solution properties. In addition to the temperature dependence of these parameters for dilute solutions, the temperature dependence of an entanglement density index in the semi-dilute concentration range will be estimated.

EXPERIMENTAL

Preparation of biopolymer samples

The polymer products were all received as fermentation broths except for one scleroglucan sample (scleroglucan A) which was delivered as a dried powder. The powder (scleroglucan A) was hydrated according to the supplier's recommendations. The polymer samples delivered as fermentation broths were routinely diluted to 5·0 mg/ml stock solutions using high shear mixing. Slow hydration overnight of the fermentation broth or the high shear mixing dilution method, yielded no significant difference in the measured intrinsic viscosities, thus polymer degradation was not found to occur under the applied mixing conditions. The solvent was synthetic seawater with the composition given in Table 1. The solutions were prepared from analytical quality reagents. The selected salt composition is close to that used in the injection water of many North Sea oil fields. The selected final polymer concentrations were prepared from the polymer stock solutions by further dilution with synthetic seawater. The mixing procedure was designed to simulate field operation conditions making use of in-line injection. The majority of the experiments were performed on samples prepared this way. One series of experiments was carried out to examine the influence of salinity on the rheological properties of xanthan (a separate batch of xanthan C, designated xanthan C-2). In these

Table 1. Composition of synthetic seawater

	Concentration	
	mg/liter	mmol/liter
Cations		
Na^+	11 090	482·3
K^+	460	11·8
Ca^{2+}	428	10·7
Mg^{2+}	1 368	56·3
Ba^{2+}	0	0
Sr^{2+}	8	0·09
Anions		
Cl^-	19 700	555·7
SO_4^{2-}	2 960	30·8
Total	36 014	

experiments the fermentation broths were diluted to 0·4 mg/ml polymer in 5 g/liter NaCl and clarified by successive filtrations through a package of Millipore filters with pore sizes 3 μm, 1·2 μm and 0·65 μm. The salinity of this filtrated stock solution was adjusted by extensive ultrafiltration. Some of the rheological data obtained on this filtrated sample (xanthan C-2) have been reported previously (Lund *et al.*, 1990).

Polymer concentrations were in general determined by first diluting the solutions with 1 M KCl. The polymer was then precipitated using iso-propanol, followed by drying and weighing of the precipitate. For samples prepared by ultrafiltration, measurements of total organic carbon (Dohrman Carbon Analyzer — DC 80) was used for the determination of polymer concentration.

Rheological characterization of biopolymer solutions

The viscosity was mostly determined using a Contraves Low Shear 30 viscometer. The measurements were performed by operating the instrument both manually and in automatic mode. The $\dot{\gamma}$-range used was 0·5–100 s^{-1}, and the temperature range, 20–70°C. At the higher temperatures the measurement cycle could be carried out in such a manner that the effect of evaporation on the viscosity measurements was less than 1%. Measurements at low shear rates (0·5–20 s^{-1}) and at low polymer concentrations were also carried out using a Cartesian diver viscometer (Stokke & Elgsaeter, 1981). The Cartesian diver instrument is based on two concentric cylinders, the outer (diameter 7 mm) is stationary, while the inner consists of an inverted tube (diameter 5 mm) fully immersed in the sample. A torque is applied electromagnetically to the inner cylinder. The rotation is measured using polarized light. The present version is similar to that described by Troll *et al.* (1980). The Cartesian diver instrument gives very accurate data for polymer concentrations with relative viscosities η_{rel} less than 5.

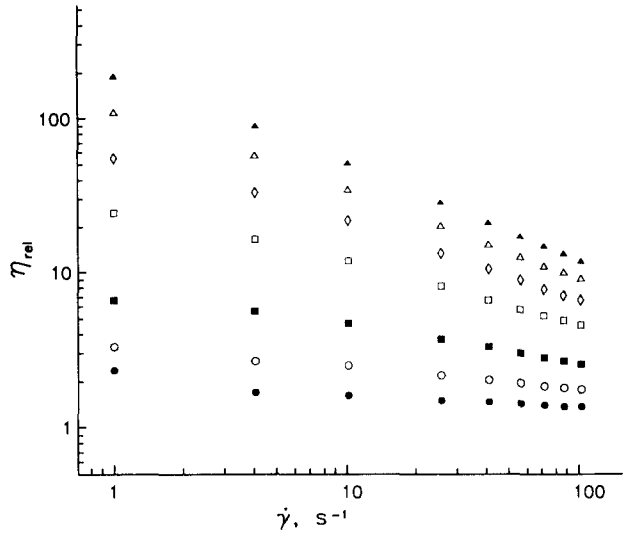

Fig. 1. Relative viscosity η_{rel} versus shear rate $\dot{\gamma}$ for c = 0·05 (●), 0·1 (○), 0·2 (■), 0·4 (□), 0·6 (◊), 0·8 (△) and 1·0 (▲) mg/ml of xanthan A in synthetic seawater measured at 20°C using the Contraves low shear viscometer.

Figure 1 shows the relative viscosity η_{rel} versus shear rate $\dot{\gamma}$, for xanthan A. The measurements were carried out for concentrations ranging from 0·05 to 1·0 mg/ml and at a temperature of 20°C. These data show that the polysaccharide solutions studied are strongly shear thinning and that the shear thinning effect is increasing with polymer concentration. The data for the other biopolymer samples displayed analogously shear-thinning and concentration dependence. It is also evident that a $\dot{\gamma}$ of about 1 s^{-1} is not sufficiently low to correspond to the lower Newtonian plateau for concentrations larger than 0·20 mg/ml for this xanthan. The present observations are in agreement to those reported by others (Whitcomb & Macosko, 1987; Milas *et al.*, 1985; Rochefort & Middleman, 1987; Allain *et al.*, 1988). The $\dot{\gamma}$ needed to reach the lower Newtonian plateau has previously been reported to be as low as $\dot{\gamma} = 10^{-1}$ s^{-1} for a 1·0 mg/ml xanthan sample having M_w = 7·0 10^6 g/mol and $[\eta]$ = 10 500 ml/g (Milas *et al.*, 1985).

Figure 2 shows the concentration dependence of η_{rel} at shear rates 1 s^{-1} to 2 s^{-1} at room temperature for the samples studied. Data obtained using the Cartesian diver instrument and the Contraves low shear instrument agree, thus giving confidence to the experimental data. Figure 2 further shows that there is a difference among the various polymers in increasing the viscosity of synthetic seawater at low shear rates with scleroglucan A being the most effective per unit mass and xanthan C the least effective. However, because in oil-field applications long-term thermal stability and ease of filtration may be more critical than viscosity, one cannot, on the basis of these data alone (Fig. 2), establish preferences for one or the other biopolymer sample. In fact, effectiveness in increasing viscosity is

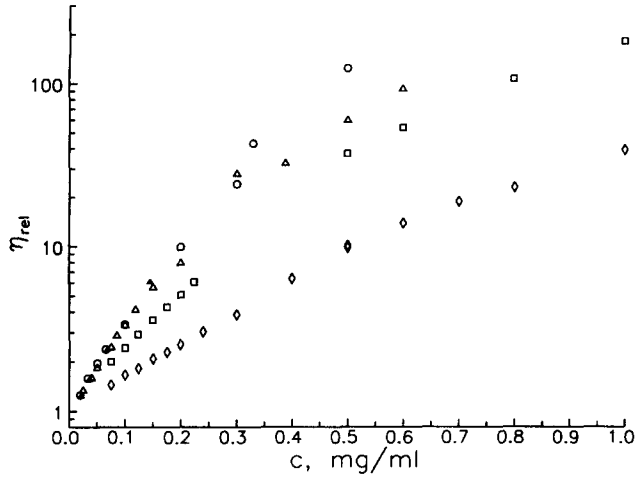

Fig. 2. Relative viscosity at low shear rate ($\dot{\gamma}$ = 1-2 s^{-1}) versus polysaccharide concentration measured at 20°C for xanthan C (◇), scleroglucan B (△) and xanthan A (□) at 30°C using the Contraves low shear instrument, at 20°C for scleroglucan A (○) and scleroglucan B (▲) using the Cartesian diver viscometer.

readily compensated for within certain limits by increasing the mass concentration whereas correction for poor filterability appear to require more elaborate methods, e.g. thermal (Holzwarth *et al.*, 1984) or enzymatic (Kohler *et al.*, 1983) treatments. The observed difference in viscosity at a certain mass concentration can be quantitated in terms of established macromolecular parameters for dilute solution viscosities and dependence of these on shear rate and temperature.

ANALYSIS OF DILUTE POLYMER SOLUTION PROPERTIES

Intrinsic viscosities, $[\eta]$, and Huggins constants, k', were calculated from experimental data for the specific viscosity, $\eta_{sp} < 1$ using several approaches. The intrinsic viscosity is conventionally obtained from the Huggins and the Kramer equations:

$$\frac{\eta_{sp}}{c} = [\eta] + k'[\eta]^2 c + O(c^2) \quad (1)$$

$$\frac{\ln(\eta_{rel})}{c} = [\eta] + (k' - 0{\cdot}5)[\eta]^2 c + O(c^2) \quad (2)$$

where c is the polymer concentration. The intrinsic viscosity was estimated as the average of the two ordinate intercepts from the two extrapolations to c = 0 mg/ml. The notation $O(c^2)$ is used to denote second and higher order terms of such power series expansion of η_{sp}/c and $\ln\eta_{rel}/c$ around c = 0 mg/ml. The slopes $\partial(\eta_{sp}/c)/\partial c$ and $\partial(\ln\eta_{rel}/c)/\partial c$ have to be divided by $[\eta]$ to yield k' (eqns (1) and (2)), thus uncertainties in the estimated $[\eta]$ propagate into uncertainties in k' in addition to those inherent in the slope. By using the inverse of the Huggins and Kramer equations:

$$\frac{c}{\eta_{sp}} = \frac{1}{[\eta]} - k'c + O(c^2) \quad (3)$$

$$\frac{c}{\ln\eta_{rel}} = \frac{1}{[\eta]} - (k' - 0{\cdot}5)c + O(c^2) \quad (4)$$

the $[\eta]$ can be estimated from the average of the two intercept at c = 0 mg/ml, and the slope provides k' directly. Mathematical formulas of viscosity where the c-dependence is less influential thereby minimizing possible errors in the extrapolation procedure to $c \to 0$ mg/ml has been suggested. Here we have included one approach applied by Lesec *et al.* (1988) in on-line viscometry of polymer samples eluted from a high performance liquid chromatography column where dilution series of each sample in practice are inaccessible:

$$[\eta]_c = \frac{(2(\eta_{sp} - \ln\eta_{rel})^{1/2}}{c} = [\eta] + O(c^2) \quad (5)$$

The first order term proportional to the polymer concentration has here been eliminated (eqn (5)), implying that the potential concentration dependence is almost neglible thus minimizing possible erroneous extrapolations. For non-associative polymer-solvent systems where k' is expected to be about 0·4, eqns (3)-(5) are preferable to eqns (1) and (2) because the extrapolation of c to 0 mg/ml represents a smaller correction to actual data and therefore the possibility of introducing erroneous corrections are less than in procedures based on eqns (1) and (2). More detailed guidelines in using different functional forms of the experimental data to obtain $[\eta]$ and k' is given by Bohdanecky and Kovar (1982).

The $[\eta]$ were calculated on the basis of eqns (1)-(5) using both a straight line and a second order polynomial in polymer concentration. For data obtained from a large number of concentrations, the evaluation of $[\eta]$ shows only a small variation (<3%) depending on the equation or the inclusion of the second order term, whereas larger variation were observed for the estimates based on fewer dilutions all corresponding to $\eta_{sp} < 1$. It was found that the sum of squared residuals was smallest when the functional form in the extrapolation was chosen either as the combination of eqns (3) and (4) or eqn (5). Averaging the $[\eta]$ estimates obtained using eqns (3), (4) and (5) results in the most consistent results within each set of data and is therefore the basis for all the intrinsic viscosity results reported here.

Figure 3 shows $[\eta]$ versus $\dot{\gamma}$ for xanthan A at different temperatures (A) and $[\eta]$ at shear rates 1-2 s^{-1} for four different sources versus temperature (B). All the samples suggest a shear rate independent Newtonian plateau of $[\eta]$ for shear rates lower than about 5 s^{-1} (Fig. 3(A) for xanthan A, others not shown), and will be

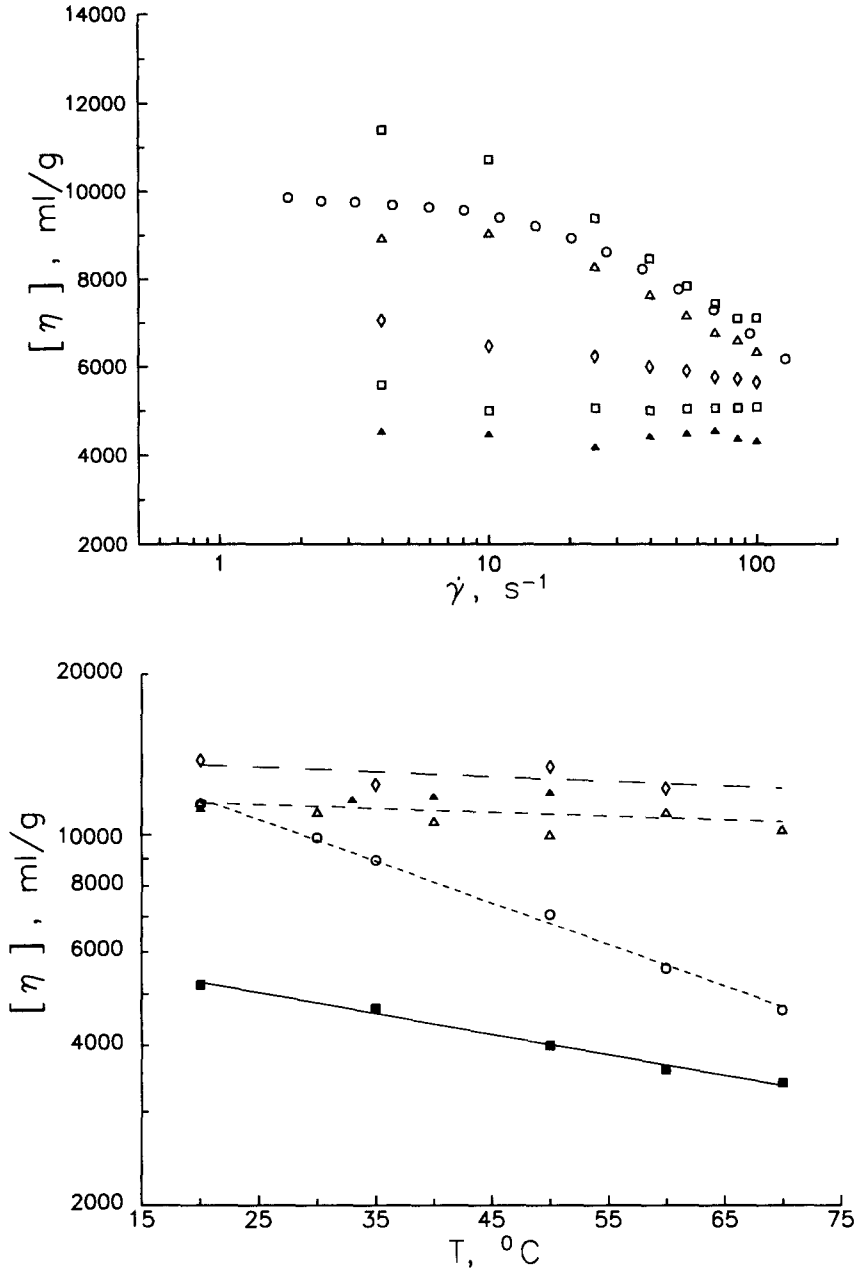

Fig. 3. (a) Intrinsic viscosity $[\eta]$ of xanthan A versus solution shear rate T = 20°C (□), 30°C (○), 35°C (△), 50°C (◇), 60°C (□) and 70°C (▲). (b) Intrinsic viscosity extrapolated to zero shear rate versus temperature for xanthan A (○), xanthan C (■), scleroglucan A (◇) and scleroglucan B (△) determined using the Contraves low shear instrument and scleroglucan B (▲) determined using the Cartesian diver instrument.

referred to as the intrinsic viscosity extrapolated to zero shear rate, $[\eta]_0$. At higher shear rates, the effect of preferred molecular orientation parallel to the streamlines leads to reduced $[\eta]$. The data does not extend into sufficient high shear rates where the second shear-rate independent plateau of $[\eta]$, $[\eta]_\infty$, is expected. The parameter $[\eta]_0$ for the samples investigated ranges from about 14 000 ml/g for scleroglucan A at $\dot{\gamma} = 1\ s^{-1}$ to 5060 ml/g for xanthan B at low temperature. These values of $[\eta]_0$ are in a range reported for other high molecular weight xanthans and scleroglucans. Differences in $[\eta]_0$ within the xanthans and the scleroglucans are most probably due to differences in apparent molecular weights and/or molecular weight distributions. Since the molecular weight distributions and corresponding averages were not determined for the present samples, detailed comparison with literature values is not warranted. On the other hand, the observed $[\eta]_0$ can be used to provide estimates of approximate molecular weights, M_w, using reported correlations between $[\eta]$ and M_w for the polymers in question. In the theory of the worm-like coil of length L, hydrodynamic diameter d and persistence length q, $[\eta]_0$ is expressed as:

$$[\eta]_0 = [\eta]_{R.0} \cdot f(L, d, q) \quad (6)$$

where $[\eta]_{R.0}$ is the intrinsic viscosity (extrapolated to zero shear rate) of a stiff rod for $L/q > 2{\cdot}278$ or a random coil-like molecule for $L/q < 2{\cdot}278$ (Yamakawa & Yoshizaki, 1980). A numerical expression of $f(L, d, q)$ and the necessary parameters are given by Yamakawa and Yoshizaki (1980).

Application of the theory for worm-like coils to experimentally determined $[\eta]$ and M_w for a series of homologous fractions of a xanthan obtained by ultrasonic irradiation, yields a persistence length of 120 nm and a hydrodynamic diameter $d = 2{\cdot}2$ nm at 20°C in 0·1 M NaCl (Sato *et al.* 1984*a*, *b*, *c*). Increasing the salt concentration further is not expected to lower the estimates of q. The contribution to q due to high structural rigidity is large compared to decreases in the electrostatic contribution to the persistence length occurring when the salt concentration is increased above 0·1 M (Tricot, 1984; Sho *et al.* 1986). This is experimentally tested for one of the samples by determining $[\eta]$ of xanthan C-2 sample at various ionic strength in mixtures of NaCl and $CaCl_2$ (Table 2). The data confirm that variations in q due to the change in Debye shielding of bound charges are not within experimental resolution for these stiff polymers at ionic strengths exceeding 0·1 M. Table 3 summarizes the intrinsic viscosity data and the estimated molecular weights of the xanthan samples applying the theory for the worm-like coil using $q = 120$ nm at $T = 20$°C, $d = 2{\cdot}2$ nm and linear mass density $M_L = 1900$ g mol^{-1} nm^{-1}. The estimated molecular weights are specified as M_w because the value of $q = 120$ nm (Sato *et al.*, 1984*a*) was based on model calculations based on experimentally determined $[\eta]$ and *weight average molecular weights* from light scattering. It does not imply that the estimated molecular weights are truly a weight average of the molecular weight distribution in the present samples. Using this approach we find estimated molecular weights ranging from $3{\cdot}5 \times 10^6$ g mol^{-1} for xanthan B to 10×10^6 g mol^{-1} for xanthan A. Analogous calculations for scleroglucan based on reported values of $q = 150$ nm, $d = 2{\cdot}6$ nm and $M_L = 2100$ g mol^{-1} nm^{-1} for schizophyllan (Kashiwagi *et al.*, 1981) and the experimental determined value of $[\eta]$ for the scleroglucan samples yielded molecular weights of 10×10^6 g mol^{-1} and 7×10^6 g mol^{-1} for scleroglucan A and B respectively (Table 3). Schizophyllan is identical in chemical composition to scleroglucan (Kashiwagi *et al.*, 1981).

Table 2. Intrinsic viscosity of xanthan C-2 in various salt solutions at $T = 20$°C

Salt composition	I	$[\eta]$ (ml/g)
5 g/litre NaCl	0·085 M	6 000
5 g/litre NaCl + 1 g/l $CaCl_2$	0·112 M	5 800
5 g/litre NaCl + 5 g/l $CaCl_2$	0·220 M	5 900
50 g/litre NaCl	0·85 M	6 000
Synthetic seawater (Table 1)	0·72 M	5 900

Figure 3(B) shows $[\eta]_0$ versus temperature in the range from 20–70°C for the polysaccharide samples studied. There is a marked difference between the xanthan samples on the one hand and the scleroglucan samples on the other. While scleroglucan samples were found to be least affected by temperatures up to about 70°C, the xanthan samples reveal a pronounced decrease in $[\eta]_0$ with increasing temperature. In fact, the observed temperature coefficients, $\partial \ln[\eta]_0/\partial T = -0{\cdot}0188$ K^{-1} (xanthan A) and $\partial \ln[\eta]_0/\partial T = -0{\cdot}009$ K^{-1} (xanthan C) are one order of magnitude larger than for most synthetic water soluble polymers (see compilation by Flory, 1969), but of the same magnitude as for derivatives of cellulose (Flory *et al.*, 1958) Xanthan C is in agreement with other reports on xanthan. Milas and Rinaudo (1986) reported $\partial \ln[\eta]_0/\partial T = -0{\cdot}008$ K^{-1} for a high molecular weight xanthan at salt conditions below the conformational transition temperature, and Kojima and Berry (1988) determined $\partial \ln[\eta]_0/\partial T = -0{\cdot}0113$ K^{-1} for a food grade xanthan having $[\eta] = 11\,300$ ml g^{-1} at 25°C in 0·62 N NaCl. Particularly, the observed temperature dependence for xanthan A is at variance with these reports. Whether this difference is due to intrinsic polymer properties or reflects temperature induced dissociation of supramolecular structures possibly remaining in the diluted fermentation broth of xanthan A is unknown. Temperature induced dissociation of supramolecular structures is actually reported to occur in a freeze-dried sample of xanthan from a specific strain (Stokke *et al.*, 1989*a*), which in that case yielded an increase in semi-dilute solution viscosity. The starting solution of that

Table 3. Molecular properties of xanthan and scleroglucan in synthetic seawater

Sample	$[\eta]_0$ (ml/g)	k′	M_w (10^6 g/mol)	$\partial ln[\eta]_0/\partial T$ (10^{-3} K^{-1})	$\partial ln q/\partial T$ (10^{-3} K^{-1})
Xanthan A	12 000	0·4	10	−18·8	−21·0
Xanthan B	5 060	0·4	3·5		
Xanthan C	5 200	0·4	3·5	−8·9	−9·4
Scleroglucan A	14 000	0·5	10	−2·0	−2·2
Scleroglucan B	11 000	0·4	7	−1·8	−2·0

particular xanthan sample and another batch of the present xanthan A, is, however, markedly different (Stokke *et al.*, 1989*b*). The observed temperature coefficient for the scleroglucan samples is $\partial \ln[\eta]_0/\partial T = -(1{\cdot}8\text{–}2.0) \times 10^{-3}\ K^{-1}$ (Table 3). This temperature coefficient is in agreement with the insensitivity of η_{sp}/c reported for a 0·72 mg/ml scleroglucan solution towards changes in temperature for the temperature range 10–70°C (Bluhm *et al.*, 1982).

The theory of worm-like coils relating $[\eta]$ to M_w enables us to transform the observed temperature coefficients of $[\eta]_0$ to temperature coefficients of q. Assuming that the molecular weight remains constant in the experimental temperature range, we used the above estimated M_w values for each sample (Table 3), a temperature independent $d = 2{\cdot}2$ nm and the experimentally determined $[\eta]_0$ at each temperature, to estimate $q(T)$. The samples were observed to be thermally stable for days below 75°C in the solvents used. The estimated temperature dependence of q observed ranges from $\partial \ln q/\partial T = -0{\cdot}021\ K^{-1}$ for xanthan A to $-0{\cdot}0094\ K^{-1}$ for xanthan C (Table 3). The values reported here can be compared to those reported by Nakasaga and Norisuye (1988). They measured $[\eta]$ for a series of homologous fractions of xanthans in 0·1 M NaCl, and the application of the theory of worm-like cylinders according to Bohdanecky (1983) yielded $q = 110 \pm 20$ nm at 25°C and $q = 70 \pm 15$ nm at 75°C for xanthan in the acid form. From these data, the temperature coefficient of q was calculated as $\partial \ln q/\partial T = -0{\cdot}0113\ K^{-1}$, which is in excellent agreement with the authors' finding for xanthan C (Table 3). The temperature coefficient of q for the scleroglucan samples were analogously estimated as $\partial \ln q/\partial T = -0{\cdot}0022\ K^{-1}$ and $-0{\cdot}0020\ K^{-1}$ for scleroglucan A and B, respectively (Table 3).

The molecular mechanism giving rise to the widely different temperature sensitivity of q between the xanthans on one hand and the scleroglucan on the other is not known. One might speculate that despite their multistranded nature, the difference in temperature sensitivity is due to the differences in proximity between the side-chains and the backbone of these two biopolymers. Xanthan has about 60% of its mass located in its side-chains, whereas in scleroglucan, merely 25% is in the branching units. If the localization of the side-chains is more crucial for the higher structural rigidity of xanthan than for scleroglucan, a strong temperature dependence of the motion of the xanthan side-chain might result in such a strong temperature dependent decrease in chain stiffness. ^{1}H NMR experiments at conditions corresponding entirely to the ordered conformation does not, however, reveal that the mobility of the xanthan side-chain substituents acetate and pyruvate are increased sufficiently to resolve changes in these signals with increasing temperature (Morris *et al.*, 1977). The small monotonous increase in the specific optical rotation occurring prior to the onset of the cooperative conformational transition (Norton *et al.*, 1984) may reflect molecular changes yielding the observed temperature coefficient in $[\eta]_0$ of xanthan. The authors are not aware of other experimental results addressing such molecular interpretations.

The numerical estimates of Huggins constant were found to be more dependent on the selected method of estimation than was the case for estimation of $[\eta]$, even when only data corresponding to $\eta_{sp} < 1$ were included in the analysis. Only k′ values obtained from estimation based on at least four polymer concentrations in this range are reported here (Table 3).

ANALYSIS OF SEMI-DILUTE POLYMER SOLUTION RHEOLOGY

Effect of polymer concentration

When the polymer concentration is increased beyond the overlap concentration, c^*, where the hydrodynamic volume of the individual chains begins to overlap, entanglement effects dominate the rheological behavior. Such entanglement effects depend strongly on shear rate even for shear rates below the critical value where the dependence of $[\eta]$ levels off at $[\eta]_0$. In the low-shear region, the observed difference in viscosity is expected to be mainly due to differences in the hydrodynamic volume among the samples. To test this the authors plotted the viscosity data as η_{rel} versus reduced concentration $c[\eta]$. Figure 4 shows η_{rel} versus reduced concentration $c[\eta]$ for each of the samples presented in Fig. 2. All data determined at this fairly low shear rate is observed to converge more or less to one single master curve. This is so even though the values of $\dot{\gamma}$ used are not sufficiently low to attain the lower Newtonian plateau for the highest polymer concentrations. The master curve for xanthan is similar to that reported by others (Shattwell *et al.*, 1990). In addition, this study indicates that the dependence of η_{rel} on reduced polymer concentration for scleroglucan is similar to that for some xanthans. This is possibly due to a similar chain stiffness for the two classes of polysaccharides at 20 and 30°C. In view of the recently reported similar plots which showed differences among xanthans having different substitutions of acetate and pyruvate or even lacking the terminal mannose in the side-chain (Shattwell *et al.*, 1990), the present finding is somewhat surprising. It might indicate that the pyruvate and acetate levels of the xanthans used are not widely different, and that the substitution levels are such that only minor differences between the xanthans and the scleroglucans are observed.

Two distinct regions of the master curve are clearly discernible. For reduced concentrations $c[\eta]$ below 1

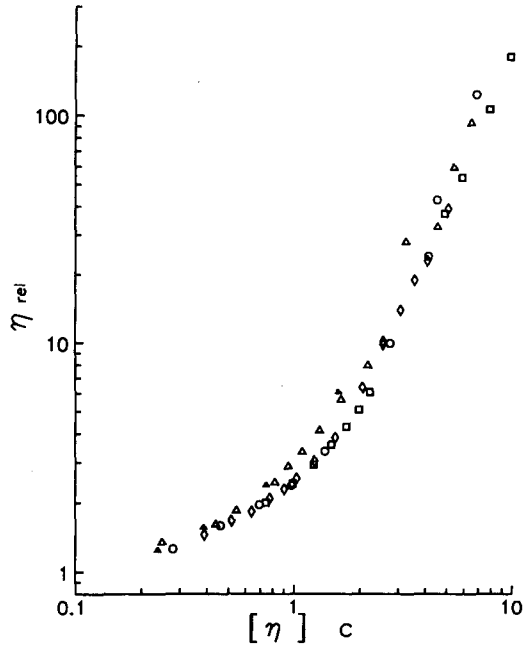

Fig. 4. Relative viscosity at low shear rate ($\dot{\gamma}$ = 1-2 s^{-1}) versus reduced polysaccharide concentration $c[\eta]$ measured at 20°C for the samples depicted in Fig. 2.

the log η_{rel} versus log($c[\eta]$) is almost linear with a slope of 0·4. Increasing the reduced concentration results in an increase of this slope ending up in a second linear region of log η_{rel} versus log($c[\eta]$) with slope of 2·3. The intercept between the extrapolations of these two straight lines is located at η_{rel} = 2·8 and $c[\eta]$ = 1·4 (Fig. 4). Although this numerical value, 1·4, of $c[\eta]$ for change of concentration regime from dilute to semi-dilute is significantly lower than 4 predicted for random coil type polymers (Graessley, 1982) and experimentally confirmed for the polysaccharide guar (Robinson *et al.*, 1982), it is in agreement with other reports on xanthan (Rinaudo & Tinland, 1989). The observed slope of 2·3, is, however, considerably less than the value of 3·4 expected for random coil type polymers. Such deviations in the present data are encountered because of the limitations introduced by the lack of the lower Newtonian plateau (Fig. 1).

Effect of shear rate

The viscoelastic nature of semi-dilute xanthan and scleroglucan solutions precludes the construction of a master curve incorporating the shear-thinning effect in a universal way from the dilute to the semi-dilute concentration range (Chauveteau, 1982). Empirical functions of various forms have been used to model the viscoelastic nature of xanthan solutions. For instance, Launay *et al.* (1984) reports better agreement between experimental data and the Cross equation with optimum adjusted parameters than the Ree-Eyring equation. The shear rate has a characteristic influence on the rheology of such oil-field biopolymers (i.e. Fig. 1) and to avoid relying on such phenomenological correlations the authors used a molecular approach to analyze shear rate effects. Figure 5 shows the reduced viscosity $\eta^* = \eta_{sp}(\dot{\gamma})/(c[\eta]_{\dot{\gamma}})$ versus the reduced concentration $c[\eta]_{\dot{\gamma}}$ with shear rates $\dot{\gamma}$ as a parameter for xanthan A and scleroglucan A at T = 20°C. The notation $[\eta]_{\dot{\gamma}}$ is used for the intrinsic viscosity at shear rate $\dot{\gamma}$ (Fig. 3). The two major features of Fig. 5 are that for $c[\eta]_{\dot{\gamma}} < 1$ the reduced viscosity η^* is only slightly dependent on $\dot{\gamma}$ whereas there is a marked sensitivity to $\dot{\gamma}$ above this reduced concentration. This behavior for $c[\eta]_{\dot{\gamma}} < 1$ is expected because the shear sensitivity for $[\eta]_{\dot{\gamma}}$ is actually deduced from the $\dot{\gamma}$-dependence of η_{sp} in this concentration range. The small differences among the slopes of Fig. 5 are due to the shear dependence of Huggins constant. The actual slope of such a graph is expected to be close to 0·4 because η_{sp} scales as the 1·4 power of the reduced polymer concentration ($c[\eta]$) in this concentration range. Adequate agreement with the 1·4 power dependence is reported for a xanthan in aqueous salt solutions (Milas *et al.*, 1985), although xanthan possesses significant chain stiffness implying that random coil behavior is not expected.

For $c[\eta]_{\dot{\gamma}} > 1$, there is an increased shear dependence due to the entanglement effects. In this graph, the authors have normalized using $[\eta]_{\dot{\gamma}}$ thereby accounting for the shear-induced orientational effects at the intramolecular level. The shear sensitivity of the intermolecular effects can then be quantitated as the slope of this graph for $c[\eta]_{\dot{\gamma}} > 2$. The sensitivity of such an entanglement density index, $\alpha = \partial \eta^*/\partial(c[\eta]_{\dot{\gamma}})$, to $\dot{\gamma}$ demonstrates the prominent influence of entanglement effects for $c > c^*$ (Fig. 6). The actual value of α is expected to approach 2·4 for randomly coiling, non-associating polymer molecules and a plateau at the low shear rate end (Graessley, 1982). There is no sign of a low-shear rate plateau in the present data (Fig. 6). The highest value, α = 1·5 at $\dot{\gamma}$ = 1 s^{-1}, and the finding that $\partial\alpha/\partial\dot{\gamma} \neq 0$ at this shear rate, shows that the Newtonian plateau is not encountered for these conditions. Departure from 2·4 in the observed α is not the only criteria that should be used since scaling coefficients in such plots could correspond to a higher value of α if the polymer departs from ideal, non-associating random-coil type polymer. Such deviations are actually reported for xanthan solutions (Milas *et al.*, 1985), where the data indicate that α could be as large as 3·24 in the Newtonian regime.

At the high shear rate end of the experiments there is less sensitivity to shear, and α approaches 0 (Fig. 6). As a consequence of this, the actual viscosity even above the apparent c^* is expected to be independent of shear rate. This is so despite the fact that no upper newtonian plateau in the intrinsic viscosity is observed for the highest shear rates (Fig. 3). Thus high-shear rate viscosities even in the semi-dilute concentration range

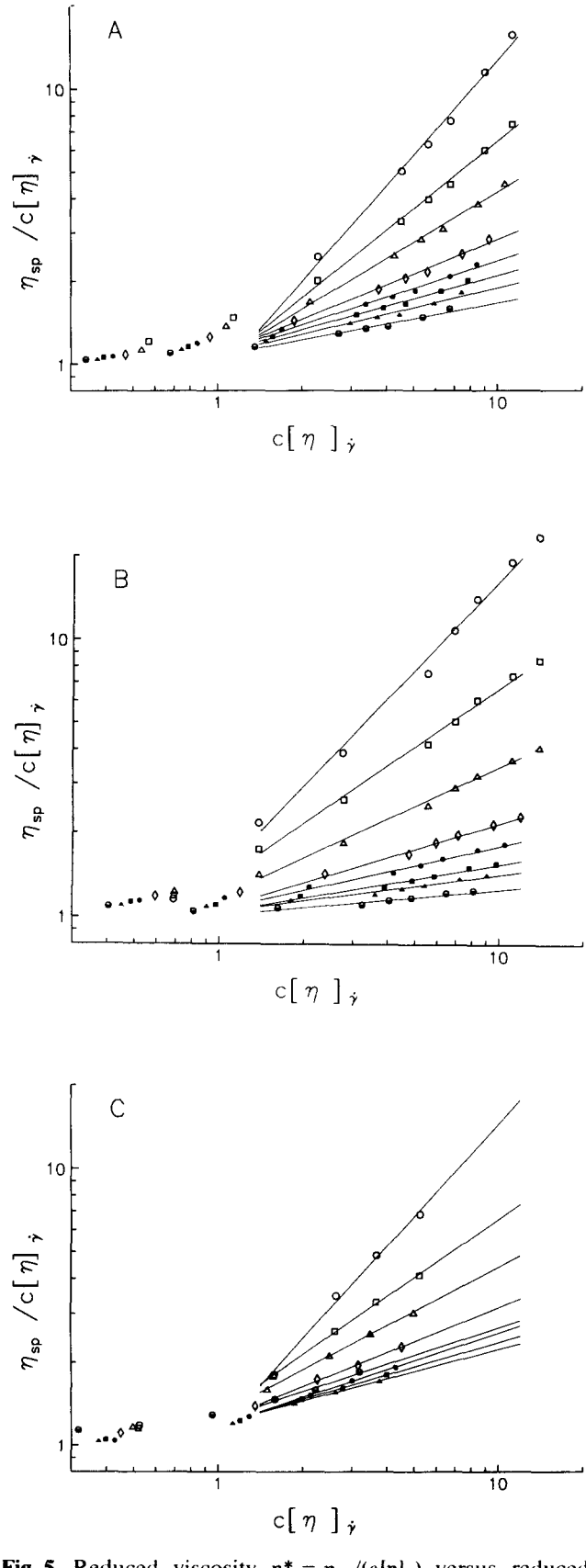

Fig. 5. Reduced viscosity $\eta^* = \eta_{sp}/(c[\eta]_{\dot\gamma})$ versus reduced polysaccharide concentration $c[\eta]_{\dot\gamma}$ for shear rate $\dot\gamma = 1\ s^{-1}$ (○), $4\ s^{-1}$ (□), $10\ s^{-1}$ (△), $25\ s^{-1}$ (◇), $40\ s^{-1}$ (●), $55\ s^{-1}$ (■), $70\ s^{-1}$ (▲) and $100\ s^{-1}$ (◒) of (a) xanthan A, (b) scleroglucan A and (c) xanthan C in synthetic seawater measured at 20°C.

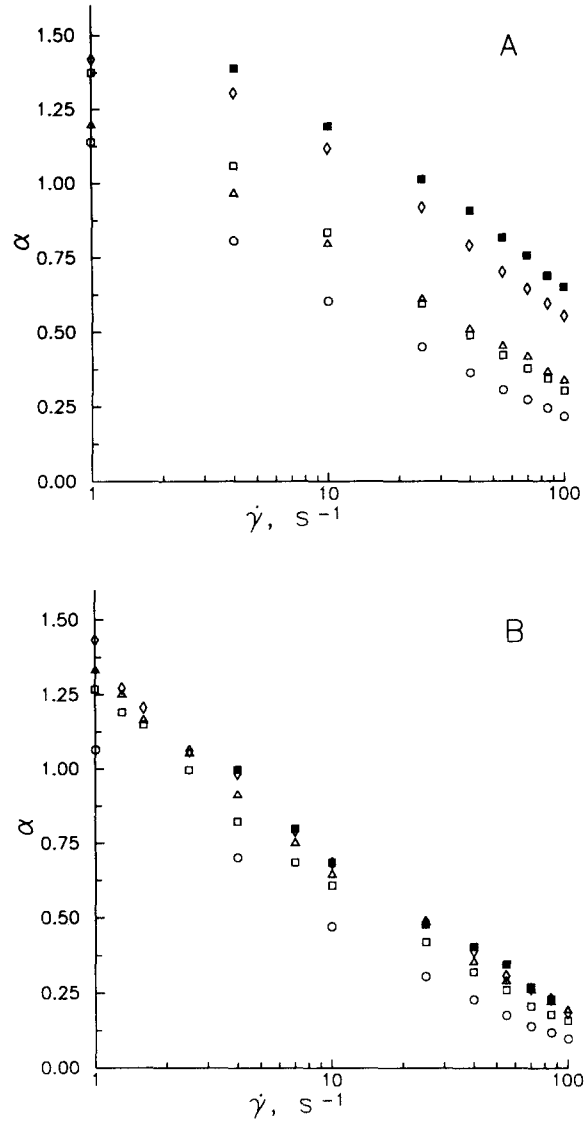

Fig. 6. Entanglement density index $\alpha = \partial\eta^*/\partial(c[\eta]_{\dot\gamma})$ versus shear rate for (a) xanthan A and (b) scleroglucan B at T = 20°C (○), 35°C (□), 50°C (△), 60°C (◇) and 70°C (■).

is calculable from the observed $[\eta]_{\dot\gamma}$, or vice versa, that $[\eta]_{\dot\gamma}$ can be evaluated from observations in the semi-dilute regime.

An additional distinct feature of the data presented in Fig. 5 is that all the lines describing the behavior of $\log\eta^*$ versus $\log c[\eta]_\gamma$ for $c[\eta]_{\dot\gamma} > 2$ at the different shear rates appear to have a common origin and intercept with the line for $c[\eta]_{\dot\gamma} < 1$. This common intercept is identical in value to the change of slopes in Fig. 4, and therefore suggests that the apparent overlap concentration at a given shear rate is related to the intrinsic viscosity at the shear rate analogous to what is seen in the Newtonian regime, i.e. $c^*(\dot\gamma) = 1{\cdot}4/[\eta]_{\dot\gamma}$ is not restricted to $\dot\gamma \to 0\ s^{-1}$, but is also valid at finite shear rates. Similar analyses at different temperatures reveal that this method yields consistent estimates of c^* independent of temperature. Attempts to fit the observed

data to a function depending on ($k'c[\eta]_{\dot\gamma}$) (Kojima & Berry, 1988) did not provide a universal curve accounting for the shear sensitivity at both dilute and semi-dilute concentrations, and will not be discussed further.

Overlap concentration and Mark-Houwink exponents

The Mark-Houwink exponent, a, relates the power law dependence of the molecular weight M of the intrinsic viscosity:

$$[\eta]_0 = K \cdot M^a \qquad (7)$$

where K is a prefactor traditionally deduced from measurements of M and $[\eta]$ for a series of homologous fractions of the polymer. The coefficients are valid over a limited range of molecular weights where log $[\eta]$ is linearly dependent on log M and is not as general as the description in terms of the worm-like cylinder referred to above (eqn (6)). However, as estimates of the a coefficient will be needed later in the discussion, we proceed as follows. It has recently been proposed that the a parameter can be deduced from the concentration dependence of η_{rel} in the semi-dilute domain (Lefebvre, 1982):

$$\ln\eta_{rel} = 2a[\eta]c^*(c/c^*)^{1/2a} - (2a - 1)c^*[\eta] \qquad (8)$$

Applied to a pectin sample, this approach yielded values for the a coefficient in reasonable agreement with the conventional approach (Axelos *et al.*, 1989). In their analysis, c^* was deduced from the deviation from the $(c[\eta])^{1.2}$ power law dependence of η_{sp}. The latter approach was implemented (eqn (8)) and employed to estimate simultaneously c^* and the a coefficient using a fixed predetermined value of $[\eta]$ and corresponding values of η_{rel} and c at the different shear rates, using non-linear regression (simplex algorithm). The values of c^* estimated in this way can then be compared with those obtained above (Fig. 4). The estimated values of c^* (Table 4) show no systematic dependence on the shear rate. The estimated product c^* $[\eta]_{\dot\gamma}$ lies in the range 0·2–0·9 for the samples listed in Table 4, and there is a clear trend of decreasing $c^*[\eta]_{\dot\gamma}$ as the shear rate increases. This contrasts with the appearance of a common intercept for all the lines deduced at different $\dot\gamma$ (Fig. 5), which indicate constancy of $c^*[\eta]_{\dot\gamma}$. The estimated values of the a coefficients are in the range 1·1–1·2 for the xanthan A sample at 20°C, decreasing to 0·6–0·7 at 70°C. For scleroglucan A it lies in the range 1·15–1·46 at 20°C decreasing to 1·05–1·2 at 60°C. The reduction in the a coefficient on increasing temperature is less for the scleroglucan than for the xanthan sample, which is in agreement with the difference in temperature coefficient of q for the two polymers (Table 3). Milas *et al.* (1985) report a = 1·14 for xanthan samples in the range M_w = (0·3–7) 10^6 g mol^{-1}, whereas Holzwarth (1978) give a = 1·35 for xanthan preparations with $M_w < 1 \times 10^6$ g mol^{-1} decreasing to a = 0·96 for $M_w > 5 \times 10^6$ g mol^{-1}. The present finding at 20°C appears to be in agreement with the former ones, whereas somewhat high relative to that reported by Holzwarth (1978) at a comparable molecular weight.

Table 4. Overlap concentrations and Mark-Houwink coefficients of xanthan A and scleroglucan A

$\dot\gamma$ s^{-1}	Xanthan A T = 20°C c* mg/ml	$c^*[\eta]_{\dot\gamma}$	a	Xanthan A T = 70°C c* mg/ml	$c^*[\eta]_{\dot\gamma}$	a
4	0·057	0·69	1·20	0·063	0·25	0·60
10	0·048	0·55	1·19	0·049	0·20	0·62
40	0·049	0·43	1·17	0·047	0·20	0·67
100	0·051	0·34	1·11	0·047	0·20	0·72
$\dot\gamma$ s^{-1}	Scleroglucan A T = 20°C c* mg/ml	$c^*[\eta]_{\dot\gamma}$	a	Scleroglucan A T = 60°C c* mg/ml	$c^*[\eta]_{\dot\gamma}$	a
4	0·046	0·64	1·46	0·071	0·87	1·04
10	0·038	0·46	1·32	0·066	0·80	1·20
40	0·035	0·40	1·26	0·038	0·46	1·18
100	0·035	0·28	1·15	0·032	0·33	1·11

Effect of temperature

Temperature effects will in the present analysis be separated into contributions of intra- and intermolecular origin, respectively. The direct effect of temperature on $[\eta]_0$ and the interpretation of this effect as a result of changes in polymer chain stiffness were discussed above. Here we discuss the semi-dilute concentration range. The entanglement density index, $\alpha = \partial\eta^*/\partial(c[\eta]_{\dot\gamma})$, was observed to never reach a constant, indicating that the lower Newtonian plateau was not contained within the experimental data. Thus, the temperature dependence of the Newtonian viscosity for $c > c^*$ cannot be discussed on the basis of the present data. Interpretation of the experimental data in terms of the van't Hof relation yielding apparent activation energies of viscous flow (Cuvelier & Launay, 1986; Kojima & Berry, 1988) therefore does not seem appropriate because data obtained at the same finite shear rate represent different departure from the Newtonian viscosity at various temperatures. An estimated apparent activation energy thus contains both a shear-rate, and $\partial\ln[\eta]_0/\partial T$ dependent contribution.

Temperature effects in the semi-dilute concentration range will therefore be analyzed on the basis of α. Figure 6 shows α versus $\dot\gamma$ for xanthan A at various temperatures. At higher temperature, particular α-values are found at higher $\dot\gamma$-values. Before we discuss the molecular interpretation of this phenomena, let us briefly return to the dilute solution regime where

temperature effects also are clearly discernible both at the onset of the shear thinning and the values of $[\eta]_0$ (Fig. 3(A)). At the *intramolecular* level such temperature effects can be given a molecular interpretation in terms of the rotational relaxation time of the polymer, τ_R. This is the basis for the method of reduced variables for temperature dependence of polymer viscoelastic data (Ferry, 1980). Deviations in $[\eta]$ from $[\eta]_0$ is encountered when the product $\dot{\gamma}\tau_R$ equals one or higher. In the former expression, the τ_R of a polymer molecule in dilute solution can be expressed as:

$$\tau_R = \frac{m[\eta]\eta_s M}{RT} \tag{9}$$

where m is a numerical constant of the order of 1 depending weakly on the polymer model, η_s is the solvent viscosity, R is the molar gas constant and T is the absolute temperature (Ferry, 1980). Of the parameters contained in eqn (9), the temperature dependence of both η_s and $[\eta]_0$ as well as the explicit appearance of temperature in the denominator contribute to the resulting total temperature effect of the onset of shear thinning. The feature that the Newtonian plateau of $[\eta]$ for xanthan extends to higher γ for higher T (Fig. 3(A)) is caused mainly by the decreasing η_s resulting in reduced rotational friction. Increasing the temperature thus requires a higher shear rate to reduce $[\eta]$ a given amount. An additional influential factor observed for the xanthans is the reduction in $[\eta]_0$ with increased temperature (Fig. 3(B)).

The considerations above are valid for the dilute regime, but can be extended to the *intermolecular* case where the rotational friction of the polymer molecules not only is influenced by solvent viscosity, but actually is dominated by entanglement effects. Morris and Ross-Murphy (1981) identify the primary relaxation time of a semi-dilute polymer solution as:

$$\tau_R = \frac{m(\eta_0 - \eta_s)M}{cRT} \tag{10}$$

where η_0 is the low-shear newtonian plateau of the polymer solution. Although τ_R is inaccessible based on the present experimental data, relative differences in τ_R as a function of temperature can be discussed based, e.g. on the shear rate where $\alpha = 1$, $\dot{\gamma}_{\alpha=1}$. Inherent in such an approach is the assumption that $\partial \log \eta / \partial \log \dot{\gamma}$ (i.e. the slope on a graph of $\log \eta$ versus $\log \dot{\gamma}$ at shear thinning shear rates) for $\dot{\gamma} > \tau_R^{-1}$ is independent of the temperature for the polymers studied. This assumption is expected to be well satisfied since the polymers over the temperature range studied, differ less than a factor of two in chain stiffness (Table 3). A power-law form of eqn (1) is adopted for the concentration dependence of η_{sp} in the semi-dilute concentration range according to Milas *et al.* (1985):

$$\eta_{sp} \sim K_n(c[\eta]_0)^n \tag{11}$$

Making the approximation that $\eta_0 \gg \eta_s$, and insertion of $\eta_0 \simeq \eta_{sp}\,\eta_s$ yields:

$$\tau_r \simeq \frac{\eta_{sp}\eta_s M}{cRT} \sim \frac{(c[\eta])^n \eta_s M}{cRT} \tag{12}$$

Using the observation that the onset of shear thinning occurs at $\dot{\gamma}\,\tau_R = 1$ and using the Mark-Houwink equation to express M in terms of $[\eta]$ (eqn (7)), the critical shear rate is found to scale as:

$$\dot{\gamma}_c \sim \frac{T}{\eta_s}[\eta]^{-(n + (1/a))} \tag{13}$$

on $[\eta]$. Considering temperature effects explicitly, eqn (13) is recast in the form:

$$\frac{\eta_s}{T}\dot{\gamma}_c \sim [\eta]^{-(n + (1/a))} \tag{14}$$

Figure 7 shows data for xanthan A and scleroglucan A plotted according to eqn (14) to obtain the scaling coefficient $n + 1/a$. Measurements at different temperatures were used to get different values of $[\eta]_0$, thus the range of $[\eta]_0$ spanned by the measurements covers less than half a decade. This imposes severe limitations on the precision obtainable in the numerical estimates of the scaling coefficient, and in fact the observed scaling coefficient in Fig. 7, of $-1{\cdot}7$, is at variance with that expected from $n + 1/a$ with parameter values inserted for n and a as obtained above. Although the numerical estimate of $n + 1/a$ is not of sufficient precision to judge the applicability of the present description, it is encouraging that the data deduced from the xanthan sample and the scleroglucan sample coincide.

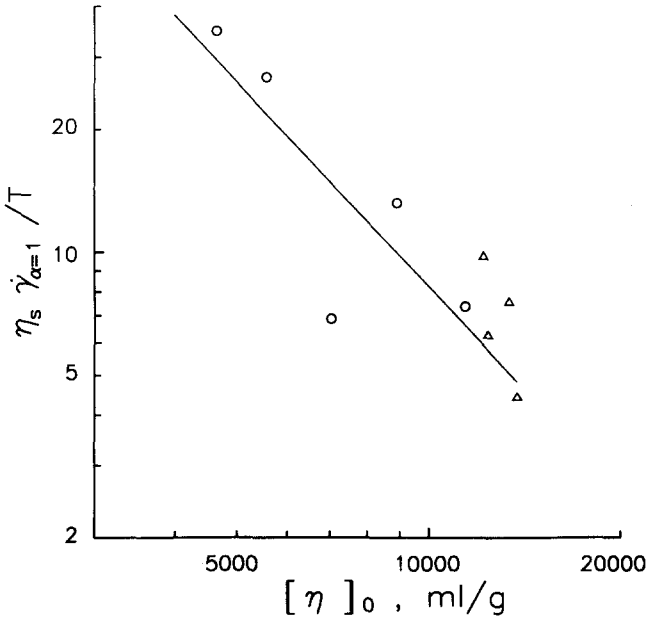

Fig. 7. Log $\eta_s\,\dot{\gamma}_{\alpha=1}/T$ (μPa K^{-1}) versus log $[\eta]_0$ obtained at different temperatures for xanthan A (○) and scleroglucan A (△).

Analysis of rheological data of xanthan and scleroglucan in synthetic seawater obtained at different polymer concentrations and shear rates indicates that chain stiffness is the basic molecular parameter altered by changes in temperature. The temperature dependence of chain stiffness is found to differ for xanthan type and scleroglucan type polymers, the latter being less temperature sensitive. The variation in temperature sensitivity within the xanthans was found to be larger than the average difference between the two types of polymers.

ACKNOWLEDGEMENTS

The authors want to thank Den norske stats oljeselskap a.s. (Statoil) for permission to publish this paper. This work was supported by grant T. 6314 from Den norske stats oljeselskap a.s. (Statoil), and VISTA, a research cooperation between the Norwegian Academy of Science and Letters, and Statoil, and grant St 10.12.220016 from the Royal Norwegian Council for Scientific and Industrial Research (NTNF).

REFERENCES

Allain, C., Lecourtier, J. & Chauveteau, G. (1988). *Rheol. Acta*, **27**, 255–62.

Axelos, M. A. V., Thibault, J. F. & Lefebvre, J. (1989). *Int. J. Biol. Macromol.*, **11**, 186–91.

Bluhm, T. L., Deslandes, Y., Marchessault, R. M., Perez, S. & Rinaudo, M. (1982). *Carbohydr. Res.*, **100**, 117–30.

Bohdanecky, M. (1983). *Macromolecules*, **16**, 1483.

Bohdanecky, M. & Kovar, J. (1982). *Viscosity of Polymer Solutions*, Elsevier Scientific Publishing, Amsterdam.

Chauveteau, G. (1982). *J. Rheology*, **26**, 111–42.

Cuvelier, G. & Launay, B. (1986). *Carbohydr. Polymers*, **6**, 321–33.

Davison, P. & Mentzer, E. (1982). *Soc. Pet. Eng. J.*, June, 353–62.

Flory, P. J. (1969). *Statistical Mechanics of Chain Molecules*, John Wiley & Sons, New York.

Ferry, J. D. (1980). *Viscoelastic Properties of Polymers*, John Wiley & Sons, New York, pp. 264–320.

Flory, P. J., Spurr, O. K. & Carpenter, D. K. (1958). *J. Polymer Sci.*, **27**, 231–40.

Graessley, W. W. (1982). *Adv. Polymer Sci.*, **47**, 67–117.

Holzwarth, G. (1976). *Biochemistry*, **15**, 4333–9.

Holzwarth, G. (1978). *Carbohydr. Res.*, **66**, 173–86.

Holzwarth, G. (1985). *Dev. Ind. Microbiol.*, **26**, 271–80.

Holzwarth, G. M., Naslund, L. A. & Sandvik, E. I. (1984). United States Patent 4 425 246.

Kashiwagi, Y., Norisuye, T. & Fujita, H. (1981). *Macromolecules*, **14**, 1220–5.

Kohler, N., Milas, M. & Rinaudo, M. (1983). *Soc. Pet. Eng. J.*, February, 81–91.

Kojima, T. & Berry, G. C. (1988). *Polymer*, **29**, 2249–60.

Lange, E. A. (1988). In *Water-Soluble Polymers for Petroleum Recovery*, ed. G. A. Stahl & D. N. Schulz, Plenum Press, New York, pp. 231–41.

Launay, B., Cuvelier, G. & Martinez-Reyes, S. (1984). *Gums and Stabilisers in the Food Industry*, **2**, 79–98.

Lefebvre, J. (1982). *Rheol. Acta*, **21**, 620–5.

Lesec, J., Lecacheux, D. & Marot, G. (1988). *J. Liq. Chromatography*, **11**, 2571–91.

Lund, T., Lecourtier, J. & Muller, G. (1990). *Polymer Degradation & Stability*, **27**, 211–25.

Milas, M. & Rinaudo, M. (1986). *Carbohydr. Res.*, **158**, 191–204.

Milas, M., Rinaudo, M. & Tinland, B. (1985). *Polymer Bulletin*, **14**, 156–64.

Milas, M., Rinaudo, M. & Tinland, B. (1986). *Carbohydr. Polymers*, **6**, 95–107.

Morris, E. R. & Ross-Murphy, S. B. (1981). *Techniques in Carbohydrate Metabolism*, **B310**, 1–46.

Morris, E. R., Rees, D. A., Young, G., Walkinshaw, M. D. & Darke, A. (1977). *J. Mol. Biol.*, **110**, 1–16.

Nakasagu, M. & Norisuye, T. (1988). *Polymer J.*, **20**, 939–44.

Norton, I. T., Goodall, D. M., Frangou, S. A., Morris, E. R. & Rees, D. A. (1984). *J. Mol. Biol.*, **175**, 371–94.

Rinaudo, M. & Tinland, B. (1989). In *Biomedical and Biotechnological Advances in Industrial Polysaccharides*, Proceedings of the 3rd International Workshop on Recent Developments in Industrial Polysaccharides: Biomedical and Biotechnological Advances, 24–26 October 1988, Trieste, Italy, ed. V. Crescenzi, I. C. M. Dea, S. Paoletti, S. S. Stivala & I. W. Sutherland, Gordon and Breach, New York, pp. 293–9.

Rivenq, R. C., Donche, A. & Noik, C. (1989). Paper presented at the 64th Annual Technical Conference and Exhibition of the Society of Petroleum Engineers, San Antonio, Texas, 8–11 October 1989, SPE preprint no. 19635, pp. 775–84.

Robinson, G., Ross-Murphy, S. B. & Morris, E. R. (1982). *Carbohydr. Res.*, **107**, 17–32.

Rochefort, W. E. & Middleman, S. (1987). *J. Rheol.*, **31**, 337–69.

Sandford, P. A., Pittsley, J. E., Knutson, C. A., Watson, P. R., Cadmus, M. C. & Jeanes, A. (1977). In *Extracellular Microbial Polysaccharides*, ACS symposium series 45, ed. P. A. Sandford & A. Laskin. ACS, Washington, DC, pp. 192–210.

Sato, T., Norisuye, T. & Fujita, H. (1984*a*). *Macromolcules*, **17**, 2696–700.

Sato, T., Kojima, S., Norisuye, T. & Fujita, H. (1984*b*). *Polymer J.*, **16**, 423–9.

Sato, T., Norisuye, T. & Fujita, H. (1984*c*). *Polymer J.*, **16**, 341–50.

Shatwell, K. P., Sutherland, I. W. & Ross-Murphy, S. B. (1990). In *Physical Networks. Polymers and Gels*, ed. W. Burchard & S. B. Ross-Murphy, Elsevier Applied Science, London & New York, pp. 315–33.

Sho, T., Sato, T. & Norisuye, T. (1986). *Biophys. Chem.*, **25**, 307–13.

Smith, I. H., Symes, K. C., Lawson, C. J. & Morris, E. R. (1981). *Int. J. Biol. Macromol.*, **3**, 129–34.

Speers, R. A. & Tung, M. A. (1986). *J. Food Sci.*, **51**, 96–103.

Stokke, B. T. & Elgsaeter, A. (1981). *Biochim. Biophys. Acta*, **640**, 640–5.

Stokke, B. T., Foss, P., Christensen, B. E., Kierulf, C. & Sutherland, I. W. (1989*a*). *Int. J. Biol. Macromol.*, **11**, 137–44.

Stokke, B. T., Elgsaeter, A. & Smidsrød, O. (1989*b*). In *Oil-Field Chemistry: Enhanced Recovery and Production Stimulation*, ed. J. K. Borchardt & T. F. Yen, Am. Chem. Soc. Symp. Ser. 396, pp. 145–56.

Tricot, M. (1984). *Macromolecules*, **17**, 1698–704.

Troll, M., Dill, K. A. & Zimm, B. H. (1980). *Macromolecules*, **13**, 436–8.

Whitcomb, P. J. & Macosko, C. W. (1978). *J. Rheology*, **22**, 493–505.

Yamakawa, H. & Yoshizaki, T. (1980). *Macromolecules*, **13**, 633–43.